

American Journal of Applied Science and Technology

# Enhancing The Efficiency Of A Tio<sub>2</sub>-Based Dye-Sensitized Solar Cell Through Ultrasonic Treatment Of The Photoanode

Sharibayev Nosir Yusupjanovich

Doctor of Physical and Mathematical Sciences, Professor, Namangan State Technical University, Uzbekistan

Ergashov Abdurasul Qodirjonovich

PhD, Senior Lecturer, Namangan State Technical University, Uzbekistan

Fazliddinov Saloxiddin Bakhriddinovich

PhD level student, Namangan State University, Uzbekistan

Received: 28 August 2025; Accepted: 24 September 2025; Published: 26 October 2025

**Abstract:** This study explores the possibility of improving the efficiency of  $TiO_2$ -based solar cells through ultrasonic treatment during the preparation of the photoanode. The article investigates the influence of ultrasonic processing of the photoanode in a solar cell fabricated with a Ru-based dye (0.3 mM N3) and an electrolyte composed of 0.05Kl + 0.10TBAl + 0.1PEO + 0.25PC + 0.25EC + 0.5DMF + 0.015l on its photoelectric performance.

**Keywords:** TiO<sub>2</sub> (titanium dioxide), DSSC (dye-sensitized solar cell), FTO (fluorine-doped tin oxide), polymer ionic electrolyte, agglomeration, deformation, cavitation, ultrasound.

## **INTRODUCTION:**

The efficiency of thin semiconductor films primarily depends on their photosensitivity and the technology used for forming the mass-transfer layer [1]. Typically, this process is based on the fabrication of thin films from a gel-like  $TiO_2$  mixture with the application of ultrasonic treatment. The process, technology, and models of  $TiO_2$  layer formation using ultrasound are discussed below [2].

The process of ultrasonic mixing is mainly associated with cavitation phenomena. Ultrasonic waves (in the frequency range of 20–100 kHz) penetrate the mixture with high energy, generating gas bubbles (cavitation cavities) [3]. When these bubbles collapse, a significant amount of energy is released, resulting in a localized increase in temperature and pressure. This promotes the breakdown of aggregated structures and creates favorable conditions for uniform particle dispersion [4].

$$E_{kav} = \frac{4}{3}\pi R^3 P_v$$

 $E_{kav}$ — energy of the cavitation bubble, R — bubble radius,  $P_v$ — internal pressure. To remove impurities and obtain  ${\rm TiO_2}$  in a gel-like state using an ultrasonic source, the following parameters are selected: ultrasonic frequency  ${\rm f_{Ut}}$ , power  ${\rm P_{Ut}}$ , and treatment time  ${\rm t_{ish}}$  [5].

The essence of obtaining TiO<sub>2</sub> in a gel-like form through the application of ultrasound lies in the following process. Under ultrasonic exposure, and due to the temperature rise caused by cavitation, the TiO<sub>2</sub> mixture transitions into a gel-like state [6]. This can be explained by the fact that, as the temperature increases, the liquid acids in the mixture gradually evaporate, which leads to an increase in the solution's density. In the gel state, it becomes possible to form a thin film characterized by high hardness and a smooth surface [7].

The general equation describing this process can be written as:

$$T_{max} = T_0 + \alpha P_{US} t_{ish}$$

where  $T_{\rm max}$  is the maximum temperature of the cavitation bubbles,  $T_0$  is the ambient temperature,  $\alpha$  is the thermal coefficient of energy generation,  $P_{US}$  is the ultrasonic power, and  $t_{ish}$  is the treatment time (s).

#### Formation of the Layer by the Spin Coating Method

To obtain high-quality thin films, the spin coating technique is widely used. In the first stage, glass substrates such as FTO and ITO are cleaned with ethanol and dried using a hot air flow device [8]. A drop of TiO<sub>2</sub> gel or an ultrasonically prepared suspension is then applied to the substrate surface. The substrate is rotated at a constant angular velocity, ensuring uniform distribution of the solution across the surface.

The technological process of spin coating, in determining the thickness of the formed layer, can be described by the following formula:

$$h(t) = h_0 exp\left(-\frac{K\eta}{\rho\omega^2}\right)$$

where h(t) is the layer thickness,  $h_0$  is the initial coating thickness, K is the geometric factor,  $\eta$  is the liquid viscosity,  $\rho$  is the liquid density, and  $\omega$  is the angular velocity of rotation (rad/s).

To prepare a mixture using ultrasound, it is essential to understand the purpose and principle of operation of the main components of the system. The frequency of the ultrasonic module should be in the range of 20–40 kHz, and the power should vary within 100–300 W [9].

Mathematically, the ultrasonic signal can be expressed as:

$$V_{in}(t) = V_0 sin(2\pi f t + \phi)$$

where  $V_0$  is the signal amplitude, f is the frequency, and  $\phi$  is the phase.

The energy of the ultrasonic signal is proportional to the power supplied to the ultrasonic source.

$$P_{US} = \frac{V_{rms}^2}{R_{load}}$$

Integration of Ultrasonic Mixing and Spin Coating Processes for Optimal Dispersion and Film Hardness. The integration of ultrasonic mixing and spin coating processes creates optimal conditions for achieving a high degree of dispersion and hardness in the resulting  $TiO_2$  coating [10].

To prepare the  $TiO_2$  mixture using the traditional method,  $4.0 \, g$  of  $TiO_2$  (Sigma-Aldrich),  $3.8 \, g$  of ethanol (98%, Uz Farm),  $0.5 \, g$  of ethyl cellulose (48.0-49.5% ethoxy groups, Sigma-Aldrich), and  $0.15 \, g$  of nitric acid (65%, Bekton) were combined with 20 mL of

ethylene. The components were weighed on high-precision electronic scales with an accuracy of up to 0.0001 g under controlled conditions [11]. The resulting mixture was stirred at room temperature for 30 minutes.

The  $TiO_2$ -containing paste was then thermally treated to remove volatile components using a rotary evaporator (IKA SMASH rotary evaporator) at 50 °C in a water bath and at 1 atm for 30 minutes [12].

For comparison with industrial products, a commercial  $TiO_2$  paste ( $TiNanoxide\ D/SP$ , Solaronix SA) was used as a reference. Two coating techniques were applied:the traditional doctor blade method (stencil deposition),

the spin coating method.

The area of the dried layers was 1.0×1.0 cm and 2.0×2.0 cm.

Glass substrates were pre-treated by immersion in a sulfochromic solution for 24 hours, followed by rinsing with distilled water and isopropyl alcohol, and drying at 100 °C [13].

To control the thickness of the applied layer, thin films of various materials were used, including adhesive tapes (up to 35  $\mu m$ ) and aluminum foils (9 and 14  $\mu m$ ). The TiO2 paste was deposited on each substrate using the doctor blade technique and then subjected to ultrasonic treatment in a bath operating at 200 W power and 20 kHz frequency for 6–200 seconds. Ultrasound was applied through probe-type transducers. The films were subsequently dried at 120 °C for 5 minutes and calcined at 350–450 °C for 30 minutes [14].

After removal from the muffle furnace, the FTO/TiO<sub>2</sub> samples were cooled to room temperature. According to the experimental plan, a Ru-based dye (0.3 mMol N3) was then prepared. The required mass of ruthenium corresponding to 0.3 mMol was weighed and dissolved in ethanol. The prepared solution was used to sensitize the photoanode consisting of FTO/TiO<sub>2</sub> [15].

This process is commonly described in the literature as the dipping method. At this stage, the photoanode and the dye solution were kept under dark conditions for several days to ensure uniform distribution of dye molecules throughout the mesoporous TiO<sub>2</sub> layer.

In thin-film solar cells, a layer that provides charge transfer and maintains electrical contact between the photoanode and counter electrode is essential. This function is performed by the electrolyte, one of the key components of the solar cell. The electrolyte composition used was as follows: 0,05KI + 0,10TBAI + 0,1PEO + 0,25PC + 0,25EC + 0,5DMF + 0,015I. The

sequence of electrolyte preparation plays a critical role, and active research is ongoing in this area.

For each series of samples, the electrolyte was subjected to ultrasonic treatment for 3, 5, and 7 minutes at temperatures of 20 °C, 50 °C, and 70 °C, respectively. The theoretical basis for selecting these conditions lies in the assumption that the transmission of low-amplitude oscillations through the liquid medium enhances catalytic activity within the system [16].

After the sample preparation stage, their electrical conductivity was analyzed. The results were represented in Nyquist coordinates.

Measurements were performed using a HIOKI IM3570 Impedance Analyzer and a BUCHI Glass Oven B-585. The samples were placed between two electrodes in compact round cells, which allowed for precise control of the measurement area and minimized errors in calculating electrical parameters.

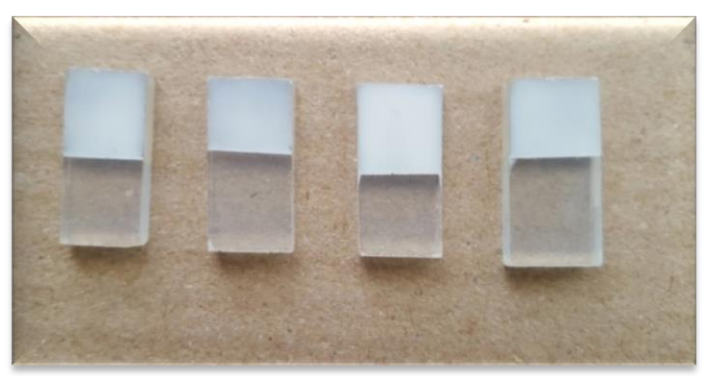


Figure 1. Unstained appearance of photoanodes fabricated using the new method.

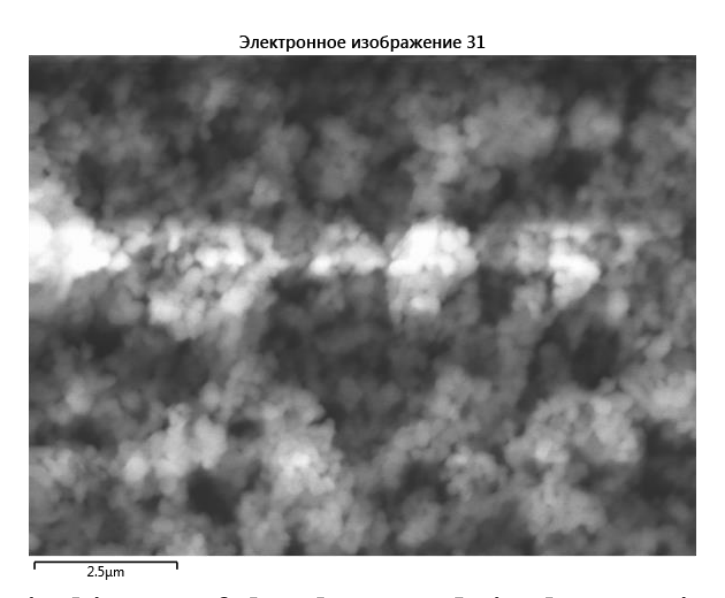


Figure 2. Morphological image of the photoanode in the unstained state obtained by SEM.

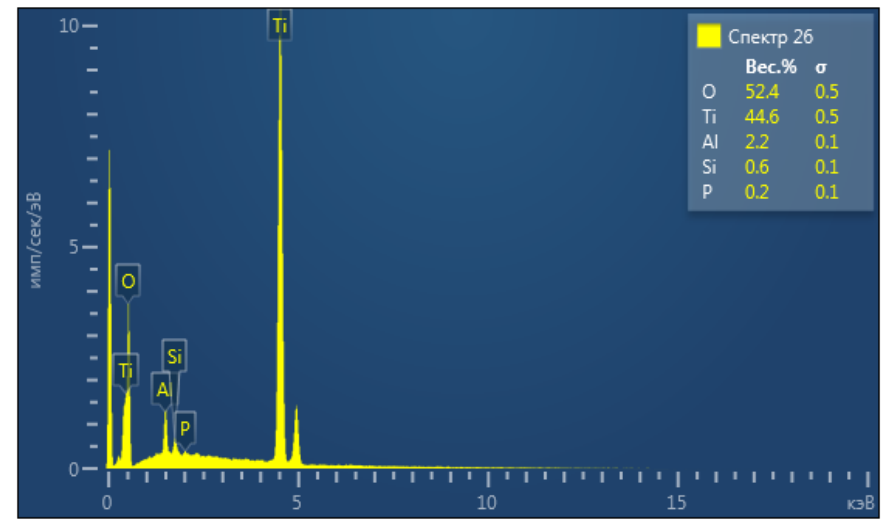


Figure 3. Spectral analysis of TiO<sub>2</sub> glass obtained by SEM.

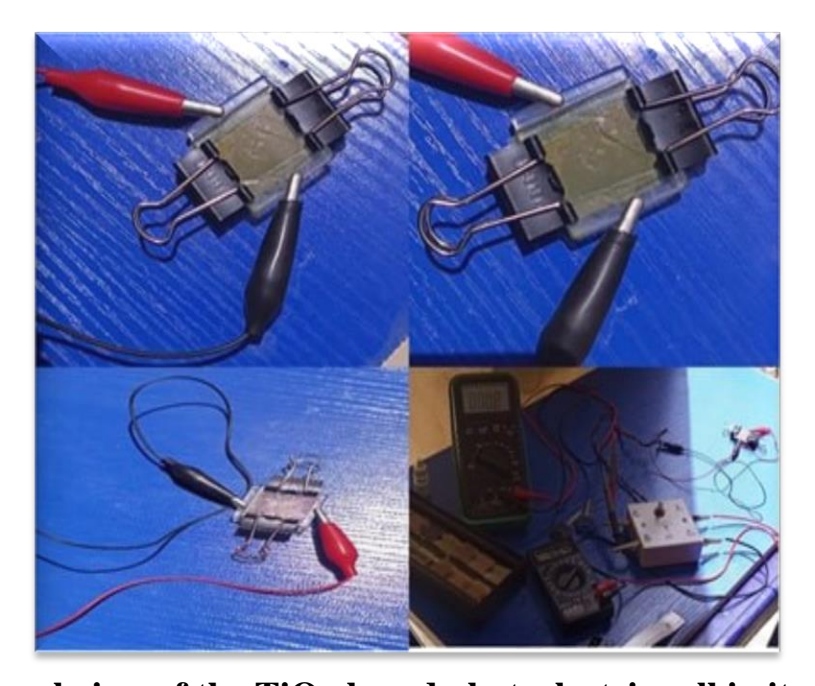


Figure 4. External view of the TiO<sub>2</sub>-based photoelectric cell in its finished state.

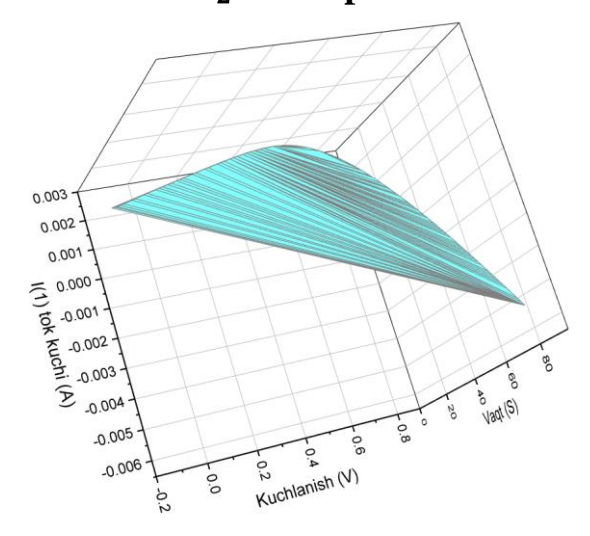


Figure 5. PhotoVAX. Measurement performed using the "Autolab" device (U = 0-0.7 V, I = 0-0.003 A).

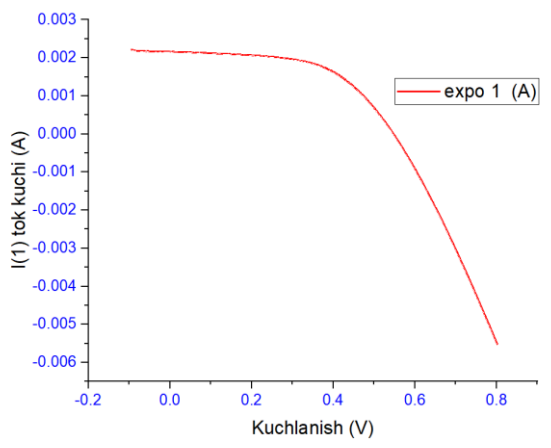


Figure 6. PhotoVAX. Autolab-UT FE with photoanode.

To initiate the experimental studies, a solar simulator was prepared. As the radiation source, the NOVA setup was selected and brought into operational condition. During the experiment, a standard illumination source **AM 1.5** with an intensity of **1000 W/m²** was used to simulate solar radiation.

In this study, the measured parameters include: Short-circuit current density (J $\mathbb{Z}$ c) mA/cm², Open-circuit voltage (Uoc) V, Fill Factor (FF), Overall efficiency ( $\eta$ ) — %.

These parameters were automatically imported into the computer system for subsequent data processing.

Table 1. Modeling the influence of dye and ultrasonic treatment on TiO<sub>2</sub>-based photoanodes based on statistical data.

| Type of Photoanode                    | <b>Ј</b> □□ (мА/ст²) | $V_o\square(V)$ | FF   | η (%) |
|---------------------------------------|----------------------|-----------------|------|-------|
| 0.3 mMol N3 dye based on Ru           | 15.55                | 0.42            | 0.72 | 5.83  |
| Ultrasound applied to the electrolyte | 17.05                | 0.42            | 0.73 | 5.84  |
| Ultrasound applied to the photoanode  | 20.05                | 0.4             | 0.75 | 5.88  |

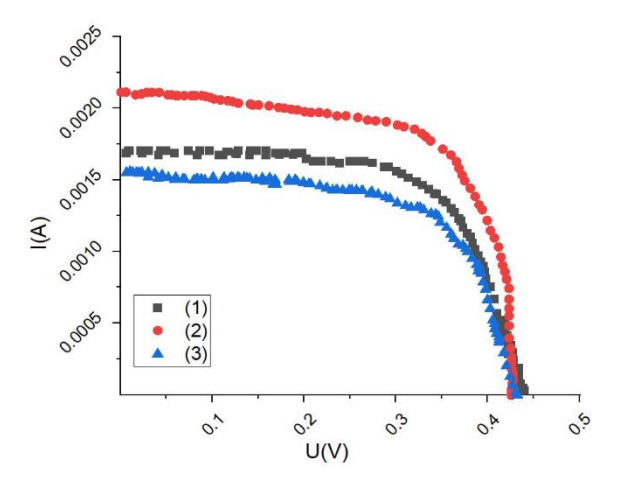


Figure 7. Effect of ultrasound on the electrolyte and photoanode of a Ru-based (0.3 mM) sample with N3 dye.

From the graph, the fill factor (FF) for the first sample was determined to be FF = 0.72. When ultrasound was applied to the electrolyte used in the same sample, the fill factor increased to FF=0.73. The highest value, FF = 0.75, was achieved when ultrasonic treatment was applied directly to the photoanode.

### **CONCLUSION**

To enhance the efficiency of dye-sensitized solar cells (DSSCs), it is essential to thoroughly investigate the

effect of ultrasonic treatment on the photoanode formation process and its influence on crystallization phenomena within the photoelectric cell.

Analysis of the presented graphs and experimental data demonstrates that applying ultrasound during the preparation of photoanodes improves structural characteristics and increases the fill factor. In particular, ultrasonic treatment during the crystallization process plays a crucial role in enhancing the structural density and surface uniformity, which in turn leads to an increase in the

overall efficiency of the solar cell.

Furthermore, the influence of ultrasound varies depending on the type of dye and its doped forms, making it important to determine the optimal parameters of ultrasonic exposure. The use of this method enables control and refinement of the crystallization process, improving the electrophysical properties and stability of the photoanodes.

Thus, the optimization of ultrasonic processing parameters represents a promising direction for improving the efficiency and manufacturing quality of dye-sensitized solar cells.

#### **REFERENCES**

- Q. A. Yousif and N. H. Haran, "Fabrication of TiO2 nanotubes via three-electrodes anodization technique under sound waves impact and use in dye-sensitized solar cell," *Egypt. J. Chem.*, vol. 64, no. 1, 2021, doi: 10.21608/EJCHEM.2020.28233.2596.
- 2. T. Rohman, A. Irwan, and Z. Rahmi, "PENURUNAN KADAR AMONIAK DAN FOSFAT LIMBAH CAIR TAHU SECARA FOTO KATALITIK MENGGUNAKAN TiO2 DAN H2O2," *J. Sains Nat.*, vol. 8, no. 2, 2018, doi: 10.31938/jsn.v8i2.156.
- **3.** S. V. Kuppu *et al.*, "The surfactants mediated electropolymerized poly(aniline) (PANI)-reduced graphene oxide (rGO) composite counter electrode for dye-sensitized solar cell," *J. Phys. Chem. Solids*, vol. 173, 2023, doi: 10.1016/j.jpcs.2022.111121.
- **4.** A. P. Kondratov, I. V. Nagornova, and L. G. Varepo, "Tenso-resistive printed sensors for flexible elements of systems and mechanisms," in *Journal of Physics: Conference Series*, 2019. doi: 10.1088/1742-6596/1210/1/012067.
- **5.** N. G. Park, "Perovskite solar cells: An emerging photovoltaic technology," 2015. doi: 10.1016/j.mattod.2014.07.007.
- **6.** J. Jenne, "Kavitation in biologischem gewebe," *Ultraschall der Medizin*, vol. 22, no. 5, 2001, doi: 10.1055/s-2001-17913.
- 7. A. Åkesson, R. Hesselstrand, A. Scheja, and M. Wildt, "Longitudinal development of skin involvement and reliability of high frequency ultrasound in systemic sclerosis," *Ann. Rheum. Dis.*, vol. 63, no. 7, 2004, doi: 10.1136/ard.2003.012146.
- **8.** S. S. Al-taweel and H. R. Saud, "New route for synthesis of pure anatase TiO2 nanoparticles via ultrasound-assisted sol-gel method," *J. Chem. Pharm. Res.*, vol. 8, no. 2, 2016.

- 9. J. Zhang, D. Liu, Y. Zhao, and S. Jiao, "Impact of heat shield structure in the growth process of Czochralski silicon derived from numerical simulation," *Chinese J. Mech. Eng. (English Ed.*, vol. 27, no. 3, 2014, doi: 10.3901/CJME.2014.03.504.
- **10.** M. Chen, K. Zhuang, J. Sui, C. Sun, Y. Song, and N. Jin, "Hydrodynamic cavitation-enhanced photocatalytic activity of P-doped TiO2 for degradation of ciprofloxacin: Synergetic effect and mechanism," *Ultrason. Sonochem.*, vol. 92, 2023, doi: 10.1016/j.ultsonch.2022.106265.
- **11.** N. M. Nursam, "PENGARUH MATERIAL COUNTER ELECTRODE PADA DYE-SENSITIZED SOLAR CELL," *Metalurgi*, vol. 34, no. 3, 2020, doi: 10.14203/metalurgi.v34i3.489.
- **12.** M. C. Lic, P. Ramón, and A. Rodríguez, "DETERMINACIÓN DE LA INFLUENCIA DEL USO DE BIODIÉSEL EN EL FUNCIONAMIENTO DE MOTORES DIÉSEL," 2010.
- **13.** W. J. Tobler and W. Durisch, "Highperformance selective Er-doped YAG emitters for thermophotovoltaics," *Appl. Energy*, vol. 85, no. 6, 2008, doi: 10.1016/j.apenergy.2007.10.006.
- **14.** H. Stanjek and W. Häusler, "Basics of X-ray diffraction," *Hyperfine Interact.*, vol. 154, no. 1–4, 2004, doi: 10.1023/B:HYPE.0000032028.60546.38.
- **15.** S. Fatimah, R. Ragadhita, D. F. Al Husaeni, and A. B. D. Nandiyanto, "How to Calculate Crystallite Size from X-Ray Diffraction (XRD) using Scherrer Method," *ASEAN J. Sci. Eng.*, vol. 2, no. 1, 2022, doi: 10.17509/ajse.v2i1.37647.
- **16.** F. I. Chowdhury *et al.*, "Electrocatalytic and structural properties and computational calculation of PAN-EC-PC-TPAI-I2gel polymer electrolytes for dye sensitized solar cell application," *RSC Adv.*, vol. 11, no. 37, 2021, doi: 10.1039/d1ra01983j.
- **17.** A. A. Hendi *et al.*, "Dye-sensitized solar cells constructed using titanium oxide nanoparticles and green dyes as photosensitizers," *J. King Saud Univ. Sci.*, vol. 35, no. 3, 2023, doi: 10.1016/j.jksus.2023.102555.
- **18.** M. K. Johari, M. A. A. Jalil, and M. F. M. Shariff, "Comparison of horizontal axis wind turbine (HAWT) and vertical axis wind turbine (VAWT)," *Int. J. Eng. Technol.*, vol. 7, no. 4, 2018, doi: 10.14419/ijet.v7i4.13.21333.
- **19.** B. Prasad, C. V. Jagtap, V. S. Kadam, S. R. Jadkar, and H. M. Pathan, "Influence of Dye Loading Time

- on Zirconia Photoanode for Solar Cell Application," *ES Energy Environ.*, vol. 20, 2023, doi: 10.30919/esee8c875.
- **20.** B. K. Ghosh, S. S. M. Zainal, K. A. Mohamad, and I. Saad, "InGaN photocell significant efficiency enhancement on Si an influence of interlayer physical properties," *Int. J. Energy Res.*, vol. 40, no. 9, 2016, doi: 10.1002/er.3520.